

## STUDY OF THE STRUCTURE OF $^{36}\text{S}$ AND $^{38}\text{Ar}$

W. S. GRAY, P. J. ELLIS †, T. WEI ††, R. M. POLICHAR and J. JÄNECKE

*The University of Michigan, Ann Arbor, Michigan 48105 †††*

Received 18 August 1969

**Abstract:** The  $^{37}\text{Cl}(d, ^3\text{He})^{36}\text{S}$  and  $^{39}\text{K}(d, ^3\text{He})^{38}\text{Ar}$  reactions have been studied at a bombarding energy of 28.9 MeV. The results are compared with theoretical calculations for two or four holes in the sd-shell. The three-hole spectrum of  $^{37}\text{Cl}$  is also briefly discussed. In the calculation for  $^{38}\text{Ar}$ , additional states of a two-particle four-hole nature are included. In  $^{38}\text{Ar}$ , the ground state and levels at 2.166 and 7.14 MeV are excited principally by  $l = 2$  transfer, while transitions with appreciable  $l = 0$  strength are observed to levels at 3.935, 4.569, 5.158 and 5.563 MeV. This fragmentation is quite well reproduced by the inclusion of the 2p–4h states. In particular the level at 3.935 MeV is largely of this type, a conclusion supported by both the spectroscopic factors and  $\gamma$  transition rates. The  $^{36}\text{S}$  ground state and levels at 6.511 and 7.12 MeV in  $^{36}\text{S}$  have angular distributions characteristic of  $l = 2$ . Three transitions with  $l = 0$  strength are observed to levels at 3.295, 4.523 and 4.577 MeV in this nucleus. An additional level was identified at 7.71 MeV but the  $l$ -transfer could not be determined. The data are only qualitatively reproduced by the four-hole calculation, which while useful in making probable  $J^\pi$  assignments, suggests that core excitation is important here also.

E

NUCLEAR REACTIONS  $^{37}\text{Cl}$ ,  $^{39}\text{K}(d, ^3\text{He})$ ,  $E = 28.9$  MeV; measured  $Q$ ,  $\sigma(E_{^3\text{He}}, \theta)$ .  
 $^{36}\text{S}$ ,  $^{38}\text{Ar}$  deduced levels,  $l_p$ ,  $J$ ,  $\pi$ ,  $S$ . Enriched  $^{37}\text{Cl}$  target.

### 1. Introduction

The  $N = 20$  nuclei  $^{36}\text{S}$  and  $^{38}\text{Ar}$  are interesting from the point of view of the shell model. In the simplest description, the low-lying, positive-parity states of these nuclei can be imagined to result from the coupling of either two or four proton holes in the 2s-1d shell. The study of their level structure might therefore be expected to yield information regarding the success of the simple shell model in the upper part of the 2s-1d shell and the extent to which excitations of the  $^{40}\text{Ca}$  core must be taken into account.

Several levels in  $^{36}\text{S}$  have been detected in a study of the  $^{34}\text{S}(t, p)^{36}\text{S}$  reaction, and the spectrum of  $^{38}\text{Ar}$  has been the subject of many experimental investigations<sup>1)</sup>. However, at the time the present work was begun, comparison between theory and experiment had been difficult because of the scarcity of experimental information regarding the configurations of the levels observed. We have studied the  $^{37}\text{Cl}(d, ^3\text{He})^{36}\text{S}$

† Present address, Rutgers, The State University, New Brunswick, New Jersey.

†† Present address, Michigan State University, East Lansing, Michigan.

††† Work supported in part by the U. S. Atomic Energy Commission and the Office of Naval Research, under Contract Nonr. 1224(59).

and  $^{39}\text{K}(d, ^3\text{He})^{38}\text{Ar}$  reactions in order to identify the levels in  $^{36}\text{S}$  and  $^{38}\text{Ar}$  which arise principally from 2s-1d configurations and to obtain spectroscopic information which can be used as a basis for detailed comparison with shell model calculations.

The  $(d, ^3\text{He})$  reaction is particularly suitable for this purpose since one expects most of the two-hole and four-hole configurations of interest to have an appreciable overlap with the removal of a proton from the respective target ground states. Also,  $(d, ^3\text{He})$  cross sections, when compared with distorted-wave predictions, have proved able to indicate satisfactorily the transferred orbital angular momentum and generally appear to provide reliable spectroscopic factors within the usual uncertainties and ambiguities associated with current distorted-wave analyses.

Preliminary results of the  $^{36}\text{S}$  experiment were reported previously <sup>2)</sup>. Recently other investigations of the  $^{37}\text{Cl}(d, ^3\text{He})^{36}\text{S}$  reaction <sup>3)</sup> and the  $^{39}(d, ^3\text{He})^{38}\text{Ar}$  reaction <sup>4)</sup> have been reported.

In sect. 5 we compare our results and those of other relevant experiments with a shell-model calculation for  $^{36}\text{S}$ ,  $^{37}\text{Cl}$  and  $^{38}\text{Ar}$  taking as a basis the  $1d_{\frac{3}{2}}$ ,  $2s_{\frac{1}{2}}$ , and  $1d_{\frac{5}{2}}$  single-particle levels. In the case of  $^{38}\text{Ar}$  core excitations of the type  $(1f_{\frac{7}{2}})^2(2s, 1d)^{-4}$  are included and found to improve agreement between theory and experiment.

## 2. Experimental procedure

The experiments were performed with 28.9 MeV deuterons from The University of Michigan 83-inch cyclotron. A preliminary investigation of the  $^{39}\text{K}(d, ^3\text{He})^{38}\text{Ar}$  reaction was also made <sup>5)</sup> at 21.1 MeV, but only the results at the higher bombarding energy are reported here.

The targets were prepared by vacuum evaporation onto thin carbon backings of KI, with the natural abundance (93.1 %) of  $^{39}\text{K}$ , and NaCl enriched to 99.3 % in  $^{37}\text{Cl}$ . The thickness of the chlorine target was determined in two ways. First, the energy lost by 8.785 MeV  $\alpha$ -particles in the target was measured and the areal density of  $^{37}\text{Cl}$  calculated under the assumption that the chemical composition of the target material (NaCl) was unchanged by the evaporation process. A second value was deduced from a measurement of the yield of deuterons elastically scattered from the chlorine component of the target in the angular range 24–32°, corresponding to the position of the secondary maximum in the elastic scattering differential cross section. The measured yield was then compared with the differential cross section predicted by the optical-model parameters used in the distorted-wave analysis. The results of the two measurements agreed within 10 % and yielded an average value of 90  $\mu\text{g}/\text{cm}^2$  for the areal density of  $^{37}\text{Cl}$  in the target.

The procedures described above were also used to measure the thickness of the potassium target, but an additional measurement was made at the conclusion of the experiment. The material on a measured area of the target was dissolved in 2 ml of water and the concentration of potassium ions in the resulting solution was measured

with an absorption spectrophotometer at The University of Michigan School of Public Health. The three determinations gave an average value of  $130 \mu\text{g}/\text{cm}^2$  of potassium with deviations of less than  $\pm 10\%$  from this value.

The probable uncertainty in the overall normalization due to uncertainties in

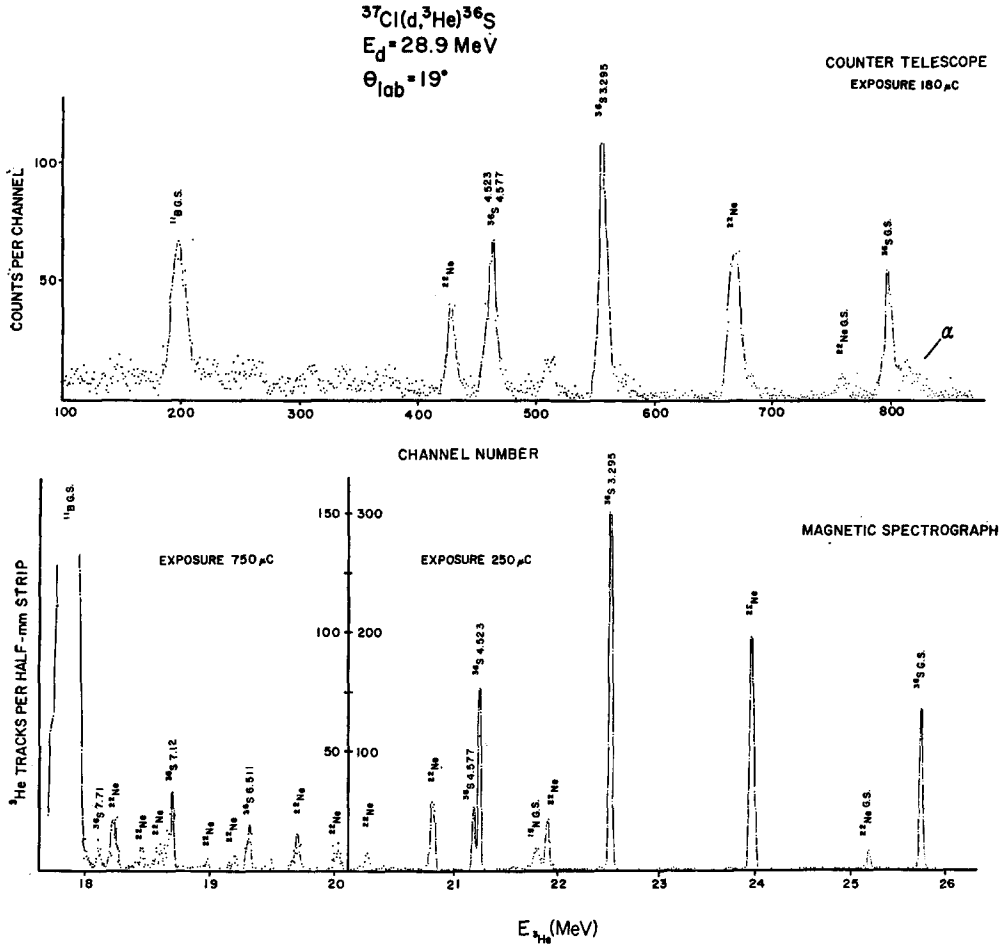


Fig. 1. Spectrum of  $^3\text{He}$  particles emitted at  $\theta_{\text{lab}} = 19^\circ$  from the  $\text{Na}^{37}\text{Cl}$  target, obtained with the counter telescope (upper half of figure) and the magnetic spectrograph (below). The spectrograph spectrum is a composite of overlapping exposures. Note that the portion of this spectrum to the left of the vertical scale marker at  $E_{^3\text{He}} = 20.1 \text{ MeV}$  was taken with a tripled beam exposure and is plotted with the vertical scale expanded by a factor of two. Apparent intensities are therefore magnified by a factor of six relative to the remainder of the spectrum.

target thickness and other factors is estimated to be  $\pm 15\%$  and  $\pm 20\%$ , respectively, for the  $^{37}\text{Cl}$  and  $^{39}\text{K}$  experiments.

Three methods were used to take the data. Except at forward angles, a  $\Delta E - E$

counter telescope was used to measure transitions to the ground state and the 3.295 MeV level in  $^{36}\text{S}$ . The  $\Delta E$  and  $E$  counters were surface-barrier detectors with nominal thicknesses of 100 and 500  $\mu\text{m}$  respectively. The signals from the two counters were fed into a pulse multiplier and a 1024-channel analyser was gated whenever the multiplier output fell within the range corresponding to  $^3\text{He}$  ions. For these events the summed  $E + \Delta E$  signal was analysed. The resolution obtained with the counter telescope was about 110 keV FWHM.

All other measurements were made with the first magnet of the three-stage magnetic spectrograph<sup>6)</sup>, as the better resolution and reduced background possible with magnetic analysis made it possible to identify much weaker transitions. At reaction angles greater than  $12^\circ$ , the  $^3\text{He}$  ions were usually detected in nuclear emulsion placed at the image surface of the spectrograph. The emulsions were Ilford type K0, 100  $\mu\text{m}$  in thickness. An aluminum absorber was placed in front of the plates to eliminate  $\alpha$ -particles and to reduce the energy of the  $^3\text{He}$  ions to the point at which they stopped in the emulsion. The  $^3\text{He}$  tracks could then be easily distinguished, on the basis of their greater density, from those due to protons and deuterons with the same magnetic rigidity.

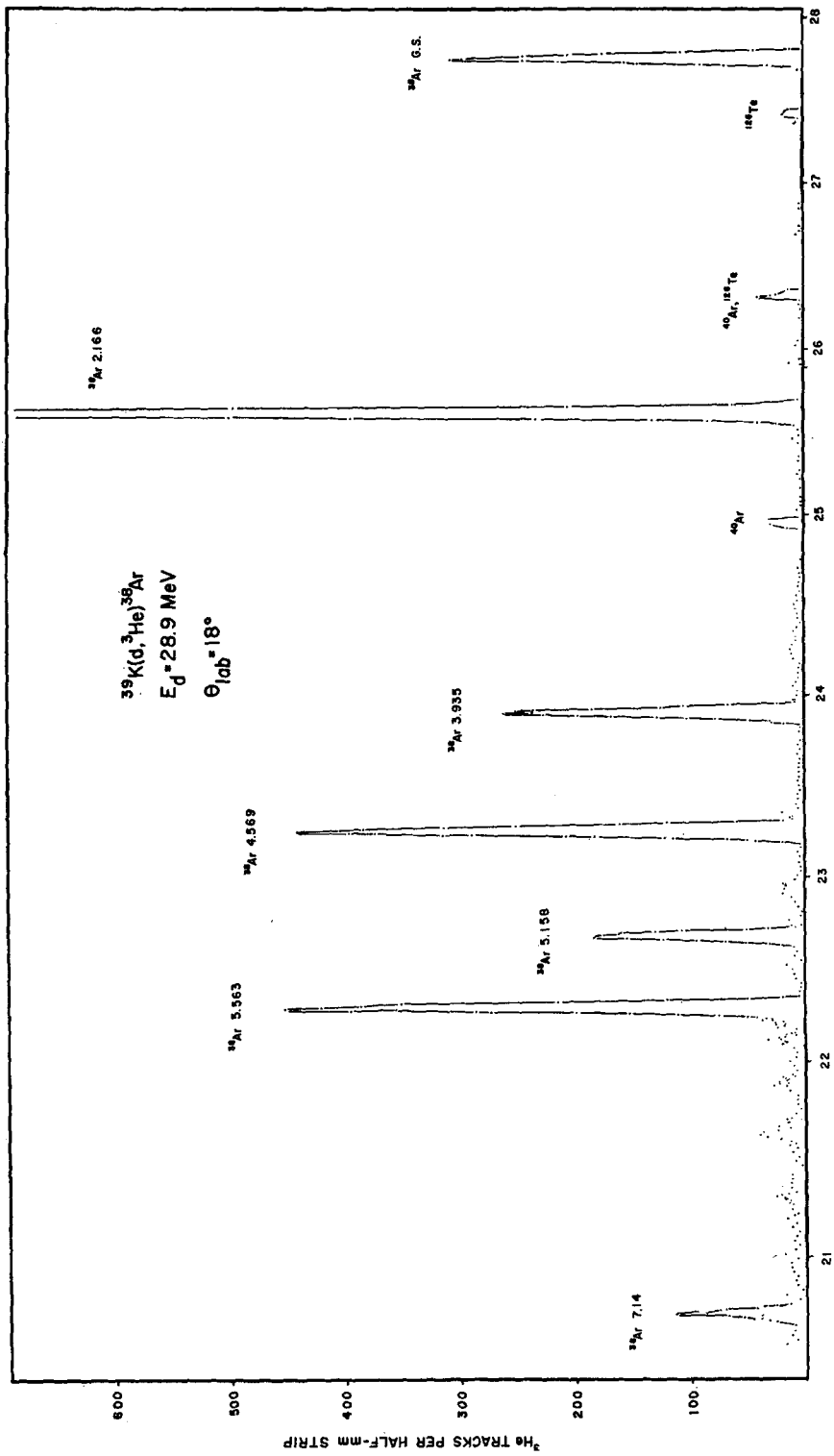
A spectrum obtained with the magnetic spectrograph for the  $^{37}\text{Cl}(d, ^3\text{He})^{36}\text{S}$  reaction is shown in the lower half of fig. 1. A spectrum taken at the same angle with the counter telescope is shown for comparison in the upper half of the figure. Groups corresponding to levels in  $^{36}\text{S}$  are labeled with excitation energies measured with the magnetic spectrograph. The doublet at 4.523 and 4.577 MeV in  $^{36}\text{S}$  was not resolved in our preliminary work and was reported as a single level at 4.57 MeV in ref. <sup>2)</sup>.

A typical spectrum obtained with the spectrograph for the  $^{39}\text{K}(d, ^3\text{He})^{38}\text{Ar}$  reaction is shown in fig. 2. Although several weak lines were observed from the  $^{127}\text{I}$  and  $^{41}\text{K}$  constituents of the target, their intensities were an order of magnitude less than those of the transitions to  $^{38}\text{Ar}$  for which angular distributions were measured.

The resolution obtained with the spectrograph was limited by target thickness to about 25 keV and 50 keV FWHM, respectively, for the  $^{37}\text{Cl}$  and potassium targets.

At reaction angles less than about  $12^\circ$  neither of the above procedures was satisfactory because of the high counting rate in the counter telescope due to elastic scattering and the presence of an intense background of low-energy deuterons at the image surface of the spectrograph. This background presumably arose from slit scattering and consisted of deuterons with approximately the same magnetic rigidity and range as the  $^3\text{He}$  ions of interest.

Since forward-angle data are important in obtaining accurate spectroscopic information from the  $(d, ^3\text{He})$  reaction, a technique was developed which allowed measurements to be made at laboratory angles greater than about  $2.5^\circ$ . Slit scattering was reduced as much as possible by removing the beam-defining slits in the scattering chamber and modifying the slit system leading to the magnetic spectrograph. Beam



$E_{^3\text{He}}$  (MeV)

Fig. 2. Spectrum of  $^3\text{He}$  particles from the  $^{39}\text{K}(d, ^3\text{He})^{39}\text{Ar}$  reaction, taken with the magnetic spectrograph at  $\theta_{\text{lab}} = 18^\circ$ .

definition and energy analysis were performed by a slit placed at the intermediate image between the two beam-preparation magnets <sup>6</sup>). Even with these precautions, however, the deuteron intensity at the most forward angles often exceeded that of the  $^3\text{He}$  ions by several orders of magnitude, making impossible an accurate count of  $^3\text{He}$  tracks in nuclear emulsions. Under these conditions, cross sections were measured with a position-sensitive detector placed at the image surface of the magnetic spectrograph. The detector used had an active area of  $14\text{ mm} \times 50\text{ mm}$  and a depletion depth of  $240\ \mu\text{m}$ . An aluminum absorber was used to maximize the energy loss of  $^3\text{He}$  ions in the detector. Since the  $50\text{ mm}$  width allowed no more than

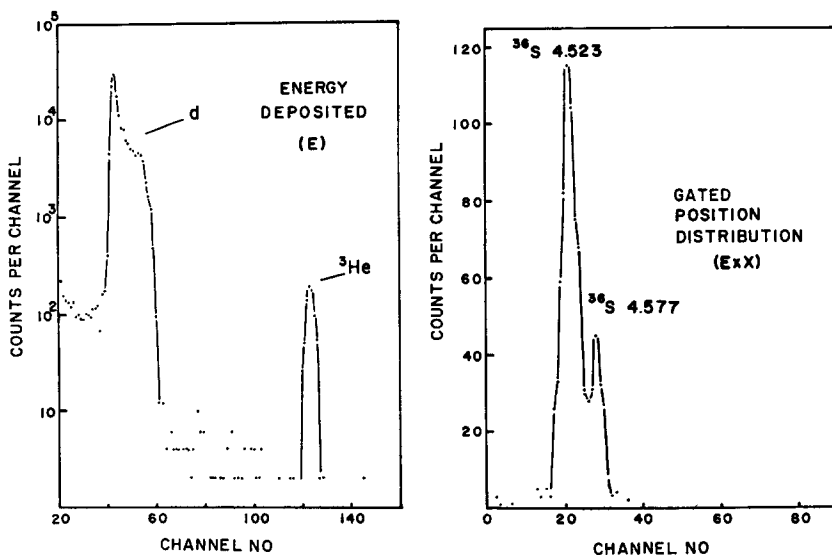


Fig. 3. Pulse-height spectrum representing energy deposited ( $E$ ) and the corresponding position spectrum ( $E \times X$ ) gated for  $^3\text{He}$  particles, obtained with a position-sensitive detector placed on the image surface of the magnetic spectrograph. The two peaks in the position spectrum represent transitions to levels at 4.523 and 4.577 MeV in  $^{36}\text{S}$ , observed at  $\theta_{\text{lab}} = 10^\circ$ .

about 500 keV of the spectrum to be covered in one exposure, transitions to single levels were usually recorded individually. For a given event, the output from the detector consisted of two signals, one proportional to the energy lost by the particle in the detector ( $E$ ), and the other proportional to the product of  $E$  and the lateral position ( $X$ ) at which the event occurred. By analysing only  $E \times X$  events for which the  $E$  signal exceeded the maximum deuteron energy it was possible to reduce the background to negligible levels. This procedure is illustrated in fig. 3, which shows an ungated  $E$  spectrum on the left and on the right the corresponding gated  $E \times X$  spectrum for the transitions to the 4.523–4.577 MeV doublet in  $^{36}\text{S}$ , taken at  $\theta_{\text{lab}} = 10^\circ$ .

Forward-angle data were taken with the Faraday cup removed from its normal position in order to allow the  $^3\text{He}$  ions to enter the magnetic spectrograph. The beam exposures for forward-angle runs were determined by monitoring the elastic scattering

from the target with a surface-barrier counter placed in the scattering chamber. The ratio of monitor events to beam exposure was checked periodically and always found to be constant within a few percent for any given set of runs.

Approximate  $Q$ -values were determined from the positions of the peaks in the spectrograph spectra and knowledge of the dispersion and momentum-versus-field relationship of the magnetic spectrograph. The excitation energy of each state was then determined more precisely by setting the magnetic field of the spectrograph to the value which would place the group corresponding to each of the preliminary  $Q$ -values at the center of the image surface. Small corrections to the excitation energies could then be made by observing the position of each group relative to that of the ground state. This procedure was calibrated by measuring the transitions to the levels <sup>1</sup>) at 1.809, 2.938, 3.940, 5.485 and 6.127 MeV in <sup>26</sup>Mg *via* the <sup>27</sup>Al(d, <sup>3</sup>He)<sup>26</sup>Mg reaction, using the precisely determined excitation energies given in ref. <sup>1</sup>). The estimated uncertainties in the measured excitation energies range from  $\pm 10$  keV, for levels below 6 MeV excitation in <sup>38</sup>Ar and <sup>36</sup>S, up to  $\pm 25$  keV for levels at higher excitation energies.

### 3. Distorted-wave analysis

Spectroscopic information was determined by comparing the measured angular distributions with non-local, finite-range distorted-wave predictions. The calculations were made with a version of the code DWUCK <sup>7</sup>), modified for use with The University of Michigan IBM 360/67 computer.

#### 3.1. SPECTROSCOPIC FACTORS

Spectroscopic strengths  $C^2S$  were obtained from the relation

$$\frac{d\sigma}{d\Omega} (\text{mb/sr}) = 29.5 \sum_{l,j} C^2 S_{lj} \frac{\sigma_{lj}(\theta)}{2j+1},$$

in which  $\sigma_{lj}(\theta)$  is the reduced cross section computed with DWUCK for pickup from the orbital ( $lj$ ),  $S_{lj}$  is the conventional spectroscopic factor <sup>8</sup>), and  $C$  is the isospin-conserving Clebsch-Gordan coefficient

$$C = \langle T | \frac{1}{2}, M_0 + \frac{1}{2} | -\frac{1}{2} | T_0 | M_0 \rangle$$

with  $T_0$  and  $T$ , respectively, the isospins of the initial and final states, and  $T_0 = M_0 = \frac{1}{2}(N-Z)$  of the target.

The factor 29.5 reflects the normalization chosen for DWUCK and includes approximation (b) of Bassel for the overlap between the d+p and <sup>3</sup>He systems <sup>9</sup>). For targets with spin  $J_0 \neq 0$  as in the present cases, the sum in the expression for the cross section extends in principle over values of ( $lj$ ) which conserve parity and can couple with  $J_0$  to the final spin  $J$ .

## 3.2. OPTICAL POTENTIALS

The optical potentials employed in the analysis were of the general form

$$U(r) = -V_0 f(x) - i[W_0 f(x') - 4W_D(d/dx')f(x')] \\ + (\hbar/m_\pi c)^2 (V_s/r) \mathbf{l} \cdot \boldsymbol{\sigma} (d/dr)f(x) + U_C(r)$$

where  $f(x)$  is  $(1 + e^x)^{-1}$ ,  $x$  is  $(r - r_0 A^{1/3})/a$ ,  $x'$  is  $(r - r'_0 A^{1/3})/a'$  and  $U_C(r)$  is the Coulomb potential due to a uniformly charged sphere of radius  $r_C A^{1/3}$ .

The parameters which were used are listed in table 1. The deuteron parameters were taken from the  $Z$ - and  $A$ -dependent average set obtained by Newman *et al.*<sup>10)</sup> in a study of 34.4 MeV deuteron elastic scattering from a range of light and intermediate nuclei. Although these parameters are appropriate for a higher bombarding energy than that of the present experiments, the lack of knowledge of the proper  $^3\text{He}$  potential is perhaps of greater concern. As there are no  $^3\text{He}$  elastic scattering data available for  $^{38}\text{Ar}$  and  $^{36}\text{S}$ , we have taken the potential used by Gibson *et al.*<sup>11)</sup> to fit the elastic scattering from  $^{40}\text{Ca}$  at  $^3\text{He}$  energies ranging from 22 to 64.3 MeV. This combination of potentials, although certainly not the optimum one, does yield distorted-wave predictions in rather good agreement with the shapes of the experimental ( $d, ^3\text{He}$ ) angular distributions.

TABLE 1  
Parameters used in the distorted-wave analysis

	$V_0$ (MeV)	$r_0$ (fm)	$a$ (fm)	$W_0$ (MeV)	$W_D$ (MeV)	$r'_0$ (fm)	$a'$ (fm)	$V_s$ (MeV)	$r_c$ (fm)
$d(^{37}\text{Cl})$	95.9	1.065	0.814	0.0	11.66	1.36	0.750	7.0	1.30
$d(^{36}\text{K})$	95.2	1.067	0.814	0.0	11.83	1.325	0.754	7.0	1.30
$^3\text{He}$	178.0	1.14	0.723	15.3	0.0	1.64	0.91	0.0	1.40
p	a)	1.20	0.65					b)	1.25

a) Adjusted to give a binding energy of  $(5.49 - Q)$  MeV.

b) Spin-orbit strength was 25 times the Thomas term.

## 3.3. BOUND-STATE FUNCTION

The wave function for the transferred proton was taken to be the eigenfunction of a Saxon-Woods potential with the depth adjusted to give binding equal to the separation energy, *i.e.*,  $5.49 \text{ MeV} - Q$  for the ( $d, ^3\text{He}$ ) reaction.

Since the magnitudes (but not the shapes) of the predicted cross sections are quite sensitive to the geometrical parameters assumed for the binding potential, uncertainties in these parameters are a major source of ambiguity in the overall normalization of spectroscopic factors obtained from distorted-wave calculations. The spectroscopic factors which we compare with theory were obtained with the radius and diffuseness parameters taken to be  $r_0 = 1.20 \text{ fm}$  and  $a = 0.65 \text{ fm}$  respectively. The Coulomb potential used in the bound-state calculation was that of a uniformly charged sphere of radius  $1.25 A^{1/3} \text{ fm}$ . These values have been used in the analysis of other



single-nucleon transfer experiments in the region around  $A = 40$  and for the most part have yielded spectroscopic factors in reasonable agreement with expectations for stripping and pickup from doubly magic targets <sup>12,13</sup>).

Spin-orbit coupling 25 times the Thomas term was included in the binding potential. The spin-orbit term has little influence upon the shapes of the predicted angular distributions in the angular range covered by the data. Its major effect is to decrease (for  $j = l - \frac{1}{2}$ ) or increase (for  $j = l + \frac{1}{2}$ ) the predicted cross section relative to the result without spin-orbit coupling, if in each case the assumed binding energy is the same. For most of the  $l = 2$  transitions encountered in the present experiments, pickup from either or both of the two 1d orbitals is in principle a possibility, depending upon the spin of the residual state. In these cases the value of  $j$  assumed in the analysis has an important bearing upon the resulting spectroscopic factor. For example, the value  $C^2S = 0.19$  obtained assuming  $l = 2, j = \frac{3}{2}$  for the transition to the level at 6.51 MeV in <sup>36</sup>S is only about 68% of the result for  $l = 2, j = \frac{5}{2}$ . The decision as to which value of  $j$  to assume in the analysis was based primarily upon the excitation energy of the particular level in question and the expectation that states with appreciable  $j = \frac{5}{2}$  strength lie at about 6 MeV or higher in <sup>36</sup>S and <sup>38</sup>Ar.

#### 3.4. CORRECTIONS FOR FINITE RANGE AND NON-LOCALITY

The distorted-wave calculations employed first-order corrections for finite range and non-locality calculated in the local energy approximation <sup>14</sup>). These corrections appear as radial damping factors applied to the distorted waves and the form factor of the usual local, zero-range (L/ZR) calculation, and have the effect of reducing the relative contributions from the nuclear interior. The application of the local-energy-approximation corrections to the (d, <sup>3</sup>He) reaction has been discussed elsewhere <sup>13</sup>).

The finite-range correction factor used in DWUCK has the form

$$W(r) = [1 + X(r)]^{-1},$$

where for the (d, <sup>3</sup>He) reaction

$$X(r) = (R^2 M_d M_p / 2\hbar^2 M_{\text{He}}) [U_{\text{He}}(r) - U_p(r) - U_d(r) - S_{\text{He}}].$$

Here  $M_i$  is the mass of particle  $i$  expressed in appropriate units,  $U_i(r)$  is the corresponding optical potential (for the proton, the binding potential),  $S_{\text{He}}$  is the separation energy of the proton from <sup>3</sup>He, and  $R$  is the range parameter as defined in ref. <sup>9</sup>), from which we take the value 1.54 fm for the (d, <sup>3</sup>He) reaction or its inverse. The approximation is most valid when the quantity  $X(r)$  is small compared to unity, a condition which is satisfied when  $U_{\text{He}} \approx U_d + U_p$  as is the case for the potentials used here.

The correction factor for non-locality is of the form

$$N_i(r) = \left[ 1 - \frac{M_i \beta_i^2}{2\hbar^2} U_i(r) \right]^{-\frac{1}{2}},$$

where  $\beta_i$  is the non-locality range parameter,  $M_i$  the mass, and  $U_i(r)$  the equivalent local optical potential for particle  $i$ .

In principle three such factors enter the transition matrix element, one each for the incoming and outgoing optical channels, and one for the bound-state function. However it has been suggested<sup>13,15)</sup> that in view of our present lack of knowledge of the energy dependence of the shell-model potential it may be more appropriate to apply these corrections only to the scattering functions, for which an estimate of the range parameter  $\beta_i$  may be deduced from the observed energy dependence of the corresponding optical potential. For this reason we have chosen to omit the non-locality correction for the bound state. Had we included it, the result would be a nearly uniform reduction of approximately 25 % in the resulting spectroscopic factors. For the deuteron and  $^3\text{He}$  optical channels we used  $\beta_d = 0.54$  fm and  $\beta_{\text{He}} = 0.3$  fm respectively.

The results of the non-local, finite-range (NL/FR) calculations were compared with L/ZR predictions for transitions representative of the range of  $Q$ -values and  $l$ -transfers which were observed. As has been noted in previous studies of the (d,  $^3\text{He}$ ) reaction<sup>13,16)</sup>, the differences in shape between the NL/FR and L/ZR angular distributions are small, at least in the angular range containing the first two or three oscillations. The main difference between the two types of calculation is that the L/ZR reduced cross sections are smaller in magnitude and would consequently lead to spectroscopic factors increased by some 20–30 % over the NL/FR values.

#### 4. Experimental results

##### 4.1. LEVELS IN $^{38}\text{Ar}$

The angular distributions measured for transitions to levels in  $^{38}\text{Ar}$  are shown in figs. 4 and 5. The solid and dashed curves are distorted-wave predictions for the  $l$ -transfers indicated in the figures. The angular distributions are labeled with the excitation energies measured in the present experiment and in some cases differ slightly, within the estimated experimental uncertainties, from the very precise values given in ref. 1).

The transitions to the ground state, the first  $2^+$  state at 2.166 MeV, and a level at 7.14 MeV display predominantly  $l = 2$  characteristics, as can be seen in fig. 4. For the ground state and the 2.166 MeV level we obtain a combined  $C^2S_2(d_{\frac{3}{2}})$  of 3.03, close to the simple shell-model expectation of 3.00 for formation of the  $0^+$  and  $2^+$  members of the  $(d_{\frac{3}{2}})^{-2}$  configuration. While the transferred angular momentum for the ground state transition is limited to  $l = 2$  and  $j = \frac{3}{2}$  by angular momentum and parity selection rules, the  $\frac{3}{2}^+ \rightarrow 2^+$  transition to the 2.166 MeV level may proceed as well by  $s_{\frac{3}{2}}$  pickup, and a small  $l = 0$  component is predicted by structure calculations (see sect. 5 or, e.g., ref. 17). The tendency of the angular distribution for this state to rise above the pure  $l = 2$  prediction at forward angles suggests the possibility of such an admixture. The dashed curve in fig. 4 represents a mixture of  $l = 0$  and

$l = 2$  with the coefficients determined by a least-squares fitting procedure. The resulting improvement in the fit to the data is probably significant, although the  $l = 0$  strength which must be added to reproduce the forward-angle data is small and sensitive to possible discrepancies between the calculated and experimental cross sections for a pure  $l = 2$  transition. It is probably safe to conclude that an  $l = 0$  component is present, with a spectroscopic factor less than 0.1.

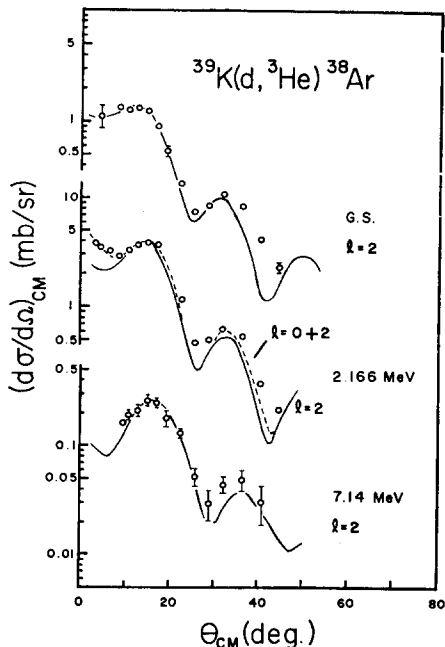


Fig. 4. Angular distributions with predominantly  $l = 2$  characteristics measured for the  $^{39}\text{K}(d, ^3\text{He})^{38}\text{Ar}$  reaction. The solid curves are distorted-wave predictions for  $l = 2$ . The dashed curve is a prediction for mixed  $l = 0$  and 2 as discussed in the text.

Since the 7.14 MeV level is at approximately the location expected for states of the  $(d_{\frac{3}{2}})^{-1}(d_{\frac{5}{2}})^{-1}$  configuration and the  $d_{\frac{3}{2}}$  strength has been exhausted, the transition to this state was analysed assuming pickup from the  $d_{\frac{3}{2}}$  orbital. With the exception of the state at 3.935 MeV, discussed below, no additional levels were excited with appreciable  $l = 2$  strength up to 8.25 MeV excitation.

Four levels were excited with appreciable  $l = 0$  strength<sup>†</sup>. The angular distributions are shown in fig. 5. Selection rules permit  $l = 2$  admixtures in these predominantly  $l = 0$  transitions, but only the angular distribution for the 3.935 MeV level shows clear evidence of  $l$ -mixing. The minimum at about  $13^\circ$  is significantly

<sup>†</sup> We take this opportunity to correct an error in ref. <sup>5</sup>), in which an additional  $l = 0$  transition to a level at 4.72 MeV was erroneously reported. A level at 4.72 MeV has therefore been listed incorrectly as  $(1, 2)^+$  in ref. <sup>1</sup>).

shallower than in the angular distributions for the 4.569, 5.158, and 5.563 MeV levels, and the prediction for pure  $l = 0$  (solid curve) falls well below the secondary maximum at  $19^\circ$  when normalized to the data forward of  $10^\circ$ . The dashed curve, which represents a mixture of  $l = 0$  ( $C^2S_0 = 0.16$ ) and  $l = 2$  ( $C^2S_2 = 0.17$ ), is in much better agreement with the data. It was obtained assuming that the angular distribution for the 4.569 MeV level has the "correct" shape for a pure  $l = 0$  transition. Use of the

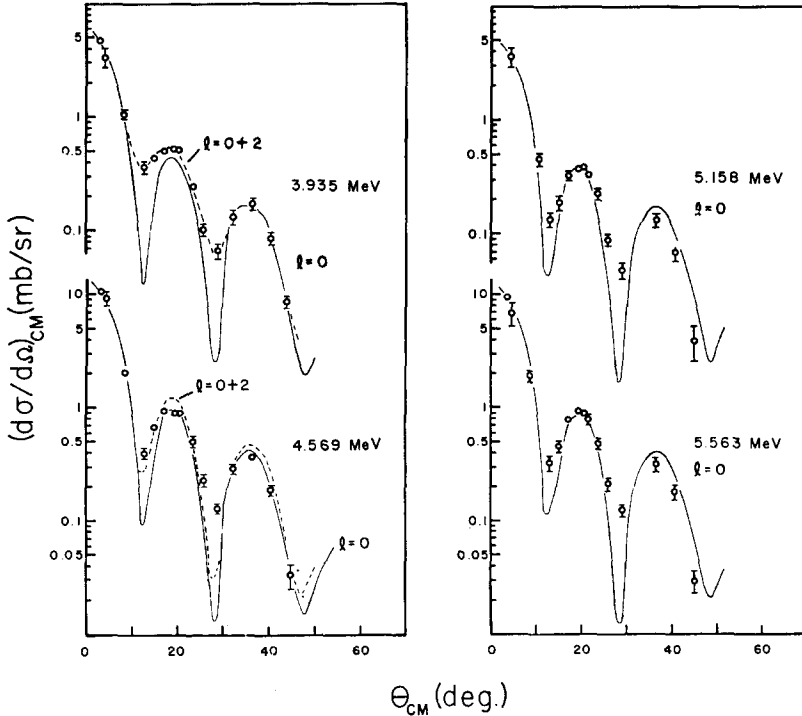
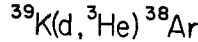


Fig. 5. Angular distributions with predominantly  $l = 0$  characteristics measured for the  $^{39}\text{K}(d, ^3\text{He})^{38}\text{Ar}$  reaction. The solid curves are distorted-wave predictions for  $l = 0$ . The dashed curves represent  $l = 0$  and 2 mixtures discussed in the text.

theoretical  $l = 0$  reduced cross section results in a somewhat poorer fit to the data but essentially the same spectroscopic factors. The  $l = 0$  strength is increased from 0.16 to 0.17 and the  $l = 2$  strength is increased from 0.17 to 0.22.

The angular distributions measured for the remaining levels at 4.569, 5.158 and 5.563 MeV are virtually identical in shape and are in good agreement with the pure  $l = 0$  predictions shown in the figure, although the minima observed at  $13^\circ$  and  $28^\circ$  are not as deep as predicted. The effect of an  $l = 2$  admixture, in the proportion  $C^2S_2 = 0.5 C^2S_0$ , is illustrated by the dashed curve drawn through the angular

distribution for the 4.569 MeV level. While the depth of the  $13^\circ$  minimum is reproduced by this mixture, the discrepancy at the second minimum remains and the relative intensities of the three observed maxima are no longer correctly predicted. It therefore seems likely that these three levels are populated by rather pure  $l = 0$  transitions, although small  $l = 2$  admixtures (probably less than 15% of the total strength) cannot be excluded.

Although there were indications in the spectrum of weak transitions to some of the known  $^1$ ) negative-parity states in  $^{38}\text{Ar}$ , none were observed at enough angles to allow clear identification in the presence of many weak groups from the  $^{127}\text{I}$  and  $^{41}\text{K}$  constituents in the target. These states would most likely be observed by  $l = 3$  pickup from particle-hole admixtures of the type  $(f_{7/2})^2(sd)^{-3}$  in the  $^{39}\text{K}$  ground state. Where possible, estimates were made of the maximum possible  $l = 3$  strength which could be attributed to each of the known levels. The results are listed in table 2.

TABLE 2  
Estimated upper limits for  $l = 3$  transfer to negative-parity states in  $^{38}\text{Ar}$

$E_x$ <sup>a)</sup>	$J^\pi$	$C^2S_3$ (max)
3.810	$3^-$	0.04
4.480	$4^-$	0.04
4.566	$(2^-)$	not resolved
4.585	$5^-$	not resolved
4.877	$3^-$	0.09
5.513	$(3^-)$	not resolved
5.658	$5^-$	0.16
6.209	$4^-$	0.08
6.601	$4^-$	0.08
6.673	$(5^-)$	0.02

<sup>a)</sup> Excitation energies and spin and parity assignments taken from ref. <sup>1)</sup>.

Only for the case of the  $5^-$  level at 5.658 MeV did the upper limit to  $C^2S_3$  exceed 0.1; in most cases the actual value is likely to be somewhat less than the estimated upper limit. The  $0^+$  state at 3.377 MeV <sup>1)</sup>, which is probably of a core-excited nature, was also not excited with detectable strength (for  $l = 2$  pickup,  $C^2S < 0.01$ ). Thus the results of the present experiment are consistent with the interpretation of the  $^{39}\text{K}$  ground state as a rather pure  $d_{3/2}$  hole state, with the likelihood of a small but non-zero particle-hole component.

The experimental results for  $^{38}\text{Ar}$  are summarized in table 3. Also given in the table are the spectroscopic strengths measured in a study of the  $^{39}\text{K}(d, ^3\text{He})^{38}\text{Ar}$  reaction at 34.5 MeV <sup>4)</sup>, together with excitation energies and spin-parity assignments taken from the compilation of Endt and Van der Leun <sup>1)</sup>. Additional levels listed in ref. <sup>1)</sup> but not observed in the  $(d, ^3\text{He})$  experiments have been omitted. Although the  $(1, 2)^+$  level determined in the present experiment to be at  $4.569 \pm 0.010$  MeV lies very close to the  $(2^-)$  level at  $4.5659 \pm 0.0005$  MeV listed in ref. <sup>1)</sup>, it appears from the

TABLE 3  
 Summary of experimental results from the  $^{39}\text{K}(d, ^3\text{He})^{38}\text{Ar}$  reaction

Level <sup>a)</sup>		Present work, (d, $^3\text{He}$ ), $E_d = 28.9$ MeV			(d, $^3\text{He}$ ), $E_d = 34.5$ MeV <sup>b)</sup>				
$E_x$	$J^\pi$	$E_x$	$l$	$J^\pi$	$C^2S_0$	$C^2S_2$	$E_x$	$C^2S_0$ <sup>c)</sup>	$C^2S_2$ <sup>c)</sup>
0	$0^+$	0	2	$0^+$		0.53	0		0.49
2.168	$2^+$	$2.166 \pm 0.010$	0, 2	$2^+$	0.05	2.50	2.17		2.50
3.377	$0^+$					<0.01			
3.936	$(2)^+$	$3.935 \pm 0.010$	0, 2	$(1, 2)^+$	0.16	0.17	3.94	0.26	0.13
4.566	$(2^-)$	$4.569 \pm 0.010$	0	$(1, 2)^+$	0.49		4.57	0.62	
$5.153 \pm 0.010$	$(1, 2)^+$	$5.158 \pm 0.010$	0	$(1, 2)^+$	0.23		5.15	0.33	
$5.551 \pm 0.010$	$(1, 2)^+$	$5.563 \pm 0.010$	0	$(1, 2)^+$	0.63		5.55	0.78	
		$7.14 \pm 0.020$	2	$(1-4)^+$		$0.40(J = \frac{3}{2})$	7.11		$0.44(J = \frac{3}{2})$
					$\Sigma C^2S_2(d_{\frac{3}{2}}) = 3.20$		$\Sigma C^2S_2(d_{\frac{3}{2}}) = 3.12$ <sup>c)</sup>		
					$\Sigma C^2S_0(s_{\frac{3}{2}}) = 1.56$		$\Sigma C^2S_0(s_{\frac{3}{2}}) = 2.00$ <sup>c)</sup>		
					$\Sigma C^2S_2(d_{\frac{5}{2}}) = 0.40$		$\Sigma C^2S_2(d_{\frac{5}{2}}) = 0.44$ <sup>c)</sup>		

<sup>a)</sup> Ref. <sup>1)</sup>. Additional levels listed in ref. <sup>1)</sup> but not observed in the (d,  $^3\text{He}$ ) experiments have been omitted. Except where noted, uncertainties in the excitation energies are less than 1 keV.

<sup>b)</sup> Ref. <sup>4)</sup>.

<sup>c)</sup> Normalized to give  $\Sigma C^2S_0 = 2.00$ .

conflicting parity assignments and other considerations to be discussed in sect. 5 that two levels exist at about this energy.

The agreement between the spectroscopic strengths measured in the present experiment and those reported in the 34.5 MeV ( $d, {}^3\text{He}$ ) study of Wildenthal and Newman <sup>4)</sup> is fairly good. The only significant difference is in the relative strengths attributed to the two observed  $l$ -transfers. As only relative cross sections were measured in the 34.5 MeV experiment, the spectroscopic factors were normalized by setting the total observed  $l = 0$  strength equal to the sum rule limit of 2.00. The value obtained

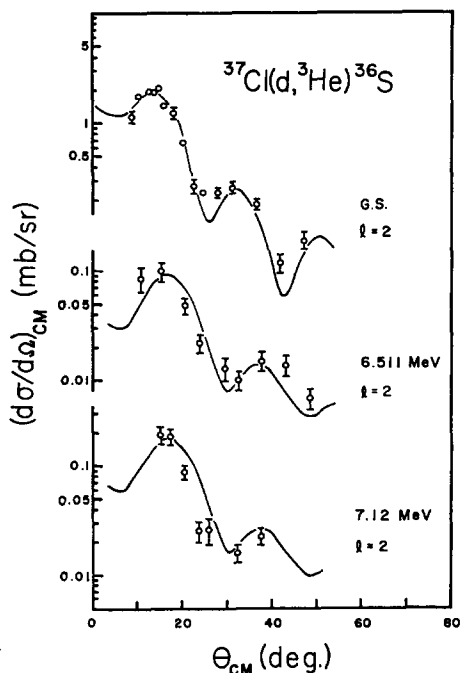


Fig. 6. Angular distributions with  $l = 2$  characteristics measured for the  ${}^{37}\text{Cl}(d, {}^3\text{He}){}^{36}\text{S}$  reaction. The solid curves are distorted-wave predictions.

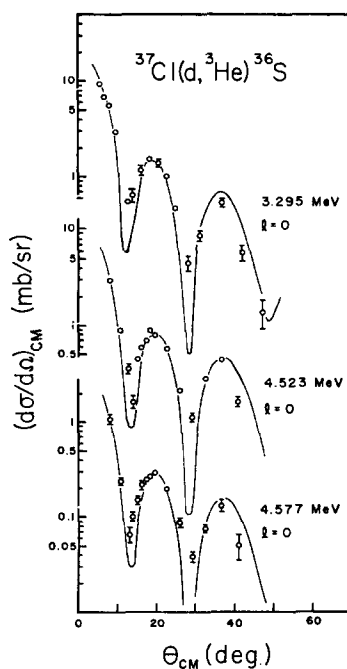


Fig. 7. Angular distributions with  $l = 0$  characteristics measured for the  ${}^{37}\text{Cl}(d, {}^3\text{He}){}^{36}\text{S}$  reaction. The solid curves are distorted-wave predictions.

for this total in the present study is 1.56. Renormalization of the spectroscopic factors of ref. <sup>4)</sup> to bring accord with this smaller total would produce excellent agreement, on a level-by-level basis, for the  $l = 0$  transitions, but would result in  $l = 2$  strengths approximately 15–25% less than our values.

#### 4.2. LEVELS IN ${}^{36}\text{S}$

Three  $l = 2$  transitions were observed to levels in  ${}^{36}\text{S}$ . The angular distributions are shown in fig. 6. The ground state transition is limited by angular momentum and parity selection rules to  $l = 2$  and  $j = \frac{3}{2}$ . The spectroscopic factor is 1.06, approximately the value expected for the total  $d_{\frac{3}{2}}$  strength. The levels at 6.511 and 7.12 MeV





are therefore probably  $d_{3/2}$  hole states, and the reduced cross sections for these levels were computed assuming pickup from that orbital. Another level at 7.71 MeV was excited too weakly to allow the transferred angular momentum to be determined. The sum of the spectroscopic factors for the 6.511 and 7.12 MeV levels is 0.63, well under the sum rule limit of 6.00 for  $d_{3/2}$  pickup. Thus, as was the case for  $^{38}\text{Ar}$ , most of the  $d_{3/2}$  strength was not observed.

The angular distributions for  $l = 0$  transitions to levels at 3.295, 4.523 and 4.577 MeV are shown in fig. 7. These three have a combined  $C^2S_0$  of 1.86, compared with the sum rule limit of 2.00.

In table 4 the results of the  $^{37}\text{Cl}(d, ^3\text{He})^{36}\text{S}$  experiment are compared with the results of a study <sup>3)</sup> of the same reaction at 23.35 MeV which has appeared subsequent to our preliminary report of the experiment <sup>2)</sup>. Additional levels observed in the  $^{34}\text{S}(t, p)^{36}\text{S}$  reaction <sup>1)</sup> are included for the sake of completeness. The levels at 4.523 and 4.577 MeV were unresolved in the 23.35 MeV experiment and can be identified with the group reported at 4.58 MeV. The strengths which were reported for the ground state, the level at 3.295 MeV, and the 4.5 MeV doublet have similar relative values but on the average are approximately 30 % greater than the values measured in the present study. This difference in normalization might be expected, since the NL/FR distorted-wave calculations we have used lead to spectroscopic factors which are approximately 25 % less than would be obtained with L/ZR calculations of the type used in ref. <sup>3)</sup>.

The authors of ref. <sup>3)</sup> have suggested, apparently on the basis of the spectroscopic factor, that the level observed by them at  $6.60 \pm 0.04$  MeV should be identified with our 7.12 MeV level, which we reported at  $7.11 \pm 0.02$  MeV in ref. <sup>2)</sup>. However we feel it is much more likely to correspond to the level at 6.511 MeV. Although the strength which they report for the 6.6 MeV level is more than a factor of four greater than we obtain for the 6.511 MeV level, the cross-section data which they measure for this weakly excited state have large errors and the spectroscopic factor is likely to be rather uncertain. Moreover, we note that the excitation energy of 6.60 MeV is based upon an energy calibration for the  $^{35}\text{Cl}(d, ^3\text{He})^{34}\text{S}$  reaction <sup>3)</sup> which in approximately this range of  $Q$ -values yields excitation energies in  $^{34}\text{S}$  that are consistently 50–80 keV higher than those measured in another study <sup>18)</sup> of the same reaction. This calibration, if corrected to agree with the excitation energies of ref. <sup>18)</sup>, would lead to approximately our measured value of 6.51 MeV.

## 5. Discussion

### 5.1. SHELL-MODEL CALCULATION

We have performed a shell-model calculation for  $^{38}\text{Ar}$ ,  $^{37}\text{Cl}$ , and  $^{36}\text{S}$ , considered as two, three, and four proton holes in the closed 2s–1d shell. The calculation was performed in the  $\text{SU}_3$  coupling scheme, afterwards transforming to the more physical  $j$ - $j$  scheme. We have used the fractional parentage coefficients of Akiyama <sup>19)</sup>,

the  $SU_3$  Clebsch-Gordan coefficients of Vergados <sup>20</sup>), and the spin-isospin fractional parentage coefficients of Jahn and Van Wieringen <sup>21</sup>).

For the single-hole energies, we take the results from the  $^{40}\text{Ca}(d, ^3\text{He})^{39}\text{K}$  reaction <sup>13</sup>), which suggest a pure  $d_{3/2}$  hole for the ground state of  $^{39}\text{K}$  and a  $d_{3/2}$ - $s_{3/2}$  splitting of 2.7 MeV. As was pointed out in sect. 4, the present experiment also suggests a rather pure  $(d_{3/2})^{-1}$  configuration for the  $^{39}\text{K}$  ground state. The authors of ref. <sup>13</sup>) estimate 6.6 MeV as a lower limit for the  $d_{3/2}$ - $d_{5/2}$  splitting, since not all of the  $d_{3/2}$  strength has been observed. We shall take a value of 7.5 MeV for this splitting in order to get approximately the correct energy for the  $d_{3/2}$  hole states observed in the present experiment.

We have taken a Yukawa interaction with a general exchange mixture

$$V_0(W + MP_x - HP_\tau + BP_o)(e^{-\rho}/\rho),$$

where  $\rho = |r_1 - r_2|/a$  and the range parameter  $a$  is taken to be 1.37 fm. The relevant exchange parameters  $V^{31}$ ,  $V^{33}$  and  $x$  are defined by

$$V^{31} = V_0(W + M - H - B), \quad V^{33} = V_0(W - M - H + B), \quad \text{and} \quad x = V^{33}/V^{31}.$$

Oscillator wave functions were used with  $\sqrt{m\omega/\hbar} = 0.52 \text{ fm}^{-1}$ . In order to determine approximately the parameters of our interaction we have varied  $V^{31}$  and  $x$  (from  $-1$  to  $+1$ ), demanding that we do not get too much binding in the ground states of either  $^{38}\text{Ar}$  or  $^{37}\text{Cl}$  and that the  $2_1^+ - 0_1^+$  splitting in  $^{38}\text{Ar}$  be  $\geq 1.6$  MeV. (The experimental value is 2.2 MeV.) These conditions allow values of  $V^{31} \approx -40$  to  $-50$  MeV with  $x \approx -1$ . We have therefore fixed  $V^{31}$  at  $-45$  MeV and  $x$  at  $-1$ . We have compared the Yukawa results with those obtained using the Kuo matrix elements <sup>22</sup>) which were calculated using realistic forces with corrections appropriate to the  $^{16}\text{O}$  core. They give reasonable results at the beginning of the  $2s-1d$  shell and we shall see that even at the end they generally give quite good answers. For the Coulomb-interaction energies of two, three, and four proton holes we have used 0.37, 1.04, and 1.87 MeV respectively, deduced from Coulomb-energy systematics.

## 5.2. TWO-HOLE CALCULATION FOR $^{38}\text{Ar}$

The spectra obtained with the two potentials are shown in fig. 8. The spectroscopic factors calculated for the Yukawa case are compared with our experimental values in table 5. The gamma transition rates calculated with this potential are compared with experiment in table 6. Similar values result for the Kuo case. The spectroscopic factors for the ground  $0_1^+$  and the first excited  $2_1^+$  states are reasonable. However, the predicted  $C^2S_0$  for the  $2_2^+$  state is much too large to be identified with the 3.94 MeV level. Also the predicted  $2_2^+ \rightarrow 2_1^+$   $B(M1)$  is an order of magnitude greater than the experimental value. A large discrepancy has also been noted in ref. <sup>23</sup>). For the E2 transitions in table 6 we have used a proton effective charge  $e_p$  of 1.5. This results in too large a  $B(E2)$  value for the  $2_1^+ \rightarrow 0_1^+$  transition and a smaller value may be more appropriate, since a coherent summation over all the terms is involved. The  $1^+$  and

second theoretical  $0^+$  states are given at rather different energies by the two potentials, reflecting differences in the diagonal  $(d_{\frac{1}{2}})(s_{\frac{1}{2}})$  and  $(s_{\frac{1}{2}})^2$  matrix elements. The  $1^+$  level is expected to have a large  $C^2S_0$  and the most likely candidate for this assignment is the level at 5.56 MeV excitation energy. The predictions are either too low (for the Kuo potential) or too high (for the Yukawa case). For the latter, fitting the 5.56 MeV

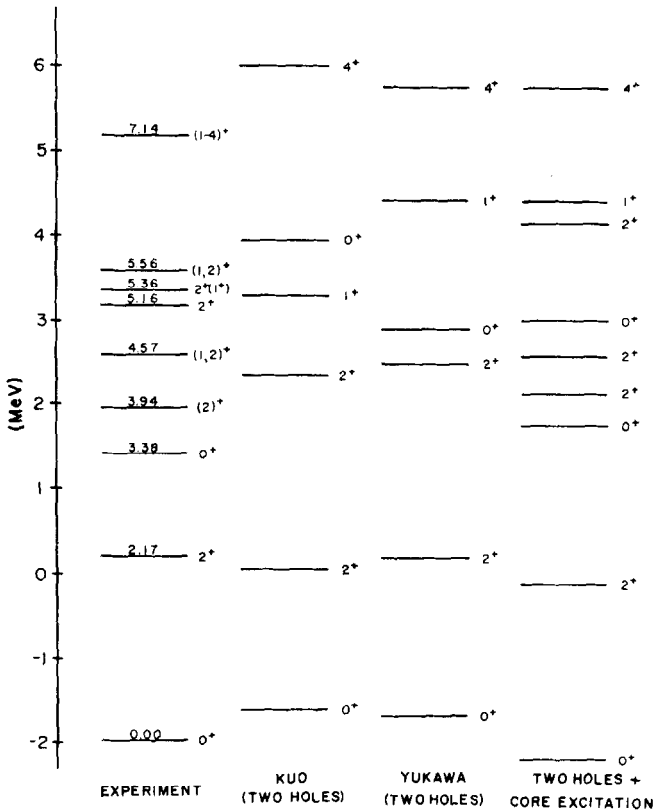


Fig. 8. Comparison of the experimentally determined positive-parity levels of  $^{38}\text{Ar}$  with the predictions of the three calculations discussed in the text. The vertical scale represents the absolute interaction energies. On this scale the ground state energy is  $2[\text{B.E.}(^{39}\text{K}) - \text{B.E.}(^{40}\text{Ca})] - [\text{B.E.}(^{38}\text{Ar}) - \text{B.E.}(^{40}\text{Ca})]$ , where the experimental values of  $\text{B.E.}(^{39}\text{K})$  and  $\text{B.E.}(^{40}\text{Ca})$  have been used.

level by adjustment of  $V^{33}$  and taking reasonable values of  $V^{31}$  leads to approximately 1 MeV too much binding in the ground state of  $^{37}\text{Cl}$ . Moinester and Alford<sup>24</sup>), using the  $^{37}\text{Cl}(^3\text{He}, d)^{38}\text{Ar}$  reaction, find a level at 6.62 MeV with  $l = (2)$  transfer which is not observed in the  $(d, ^3\text{He})$  reaction. They suggest this may correspond to the second  $0^+$ .

TABLE 5

Spectroscopic factors for the  $^{39}\text{K}(d, ^3\text{He})^{38}\text{Ar}$  reaction and intensities of core-excited configurations. The core-excited states A, B, and C are defined in the text.

Level <sup>b,c,d)</sup>	Experiment <sup>a)</sup>		Theory							
	$C^2S_0$	$C^2S_2$	two holes			two holes and core excitation				
			$J^\pi$	$C^2S_0$	$C^2S_2$	$C^2S_0$	$C^2S_2$	intensity A or B	intensity C	
G.S., $0^+$		0.53	$0_1^+$	0	0.44	0	0.39	0.13		
2.17, $2^+$	0.05	2.50	$2_1^+$	0.08	2.27	0.09	2.00	0.01	0.09	
3.38, $0^+$		<0.01	$0_2^+$			0	0.03	0.81		
3.94(2) <sup>+</sup>	0.16	0.17	$2_2^+$	1.08	0.20	0.22	0.32	0.43	0.26	
4.57(1, 2) <sup>+</sup>	0.49		$2_3^+$			0.80	0.09	0.25	0.03	
5.16, $2^+$ <sup>c)</sup>	0.23		$0_3^+$	0	0.03	0	0.04	0.06		
5.36, $2^+(1^+)$ <sup>d)</sup>										
5.56(1, 2) <sup>+</sup>	0.63		$2_4^+$			0.04	0.06	0.31	0.62	
7.14(1-4) <sup>+</sup>		0.40	$1_1^+$	0.75	0.00	0.75	0.00			
			$4_1^+$	0	2.20	0	2.20			

<sup>a)</sup> Present work.

<sup>b)</sup> Ref. <sup>1)</sup>. Only levels which have been assigned positive parity are included.

<sup>c)</sup> Present work and ref. <sup>31)</sup>, see text.

<sup>d)</sup> Ref. <sup>35)</sup>.

TABLE 6  
Reduced transition rates in  $^{38}\text{Ar}$  ( $B(\text{E}2)$  in  $e^2 \cdot \text{fm}^4$ ,  $B(\text{M}1)$  in  $e^2 \cdot \text{fm}^2$ )

transition	$\lambda$	$B(\lambda)$	transition	Theory		
				two holes	two holes and core excitation	
				$e_p = 1.5$ $e_n = 1.0$	$e_p = 1.0$ $e_n = 1.0$	
2.17 $\rightarrow$ g.s.	E2	$25 \pm 4^b$	$2_1^+ \rightarrow 0_1^+$	36	40	19
3.38 $\rightarrow$ 2.17	E2	$\leq 631$	$0_2^+ \rightarrow 2_1^+$		0.047	0.89
3.94 $\rightarrow$ g.s.	E2	$8.4 \pm 1.3$	$2_2^+ \rightarrow 0_1^+$	9.0	5.8	4.6
3.94 $\rightarrow$ 2.17	E2	$< 21$	$2_2^+ \rightarrow 2_1^+$	46	16	8.1
4.57 $\rightarrow$ g.s.	M1	$< 0.00005$	$2_2^+ \rightarrow 2_1^+$	0.0014	0.00022	0.00022
4.57 $\rightarrow$ 2.17	E2	$< 0.11$	$2_3^+ \rightarrow 0_1^+$		1.8	0.31
	E2	$20^c$	$2_3^+ \rightarrow 2_1^+$		26	11
4.57 $\rightarrow$ 3.94	M1	$0.0009^c$	$2_3^+ \rightarrow 2_1^+$		0.0015	0.0015
	E2	$< 2170$	$2_3^+ \rightarrow 2_2^+$		5.1	4.2
	M1	$< 0.0007$	$2_3^+ \rightarrow 2_2^+$		0.0054	0.0054
	M1		$2_4^+ \rightarrow 2_3^+$		0.0027	0.0027
	M1		$2_4^+ \rightarrow 2_2^+$		0.0016	0.0016

<sup>a)</sup> Ref. <sup>34</sup>).

<sup>b)</sup> H. Grawe and K. P. Lieb, quoted in ref. <sup>25</sup>).

<sup>c)</sup> Assuming  $\delta^2(\text{E}2/\text{M}1) = 0.1$ .

The low-lying states all have more than 85 % of the major  $j$ - $j$  coupled configurations, but the  $d_{\frac{3}{2}}$  configurations have a significant effect on the energies, particularly for  $J = 0$ . Of the states belonging largely to the  $(d_{\frac{3}{2}})^{-1}(d_{\frac{3}{2}})^{-1}$  configuration, the  $4^+$  lies lowest at  $\approx 8$  MeV excitation energy and the other three levels with  $J^\pi = 1^+-3^+$  lie some 2 MeV higher. These states all have  $C^2S_2 \approx \frac{1}{4}(2J+1)$ , much larger than the experimental value of 0.40 for the level at 7.14 MeV. However, at this excitation energy we would expect to find a large number of particle-hole states and presumably considerable mixing occurs. Our value for the  $d_{\frac{3}{2}}-d_{\frac{3}{2}}$  splitting therefore seems reasonable.

Excitations of the  $^{40}\text{Ca}$  core are clearly important, since starting with the  $0^+$  state at 3.38 MeV we have more levels than can be explained with a simple two-hole basis. In the following section we discuss an extended calculation in which core-excited states are included.

### 5.3. CORE EXCITATION IN $^{38}\text{Ar}$

Making use of the relevant binding energies and the monopole particle-hole interaction of Zamick <sup>25</sup>), the weak-coupling model predicts for the most favorable core excitation a state with two particles coupled to  $T = 1$  and four holes coupled to  $T = 0$ . This lies at 3.2 MeV excitation energy.

For the purpose of estimating the effects of core excitation we shall consider the ground and first excited states of  $^{42}\text{Ca}$  to be described by  $(f_{\frac{7}{2}})^2$  coupled to  $J = 0$  and 2 respectively. (We shall ignore the 0.4 MeV depression of the two-particle states found by Gerace and Green <sup>26</sup>) when four-particle two-hole (4p-2h) states are also included.) For the ground and first excited states of the four-hole,  $T = 0$  system we shall take configurations which represent over 85 % of the wave function according to Glaudemans *et al.* <sup>17</sup>). Accordingly we define three core-excited states

$$A = \left\{ \left\{ (f_{\frac{7}{2}})_{T=1}^2 (d_{\frac{3}{2}})_{T=0}^{-4} \right\}_{J=0}, \right.$$

$$B = \left\{ \left\{ (f_{\frac{7}{2}})_{T=1}^2 (d_{\frac{3}{2}})_{T=0}^{-4} \right\}_{J=2}, \right.$$

$$C = 0.78 \left\{ \left\{ (f_{\frac{7}{2}})_{T=1}^2 (d_{\frac{3}{2}} \text{ seniority } 2)_{T=0}^{-4} \right\}_{J=2} - 0.62 \left\{ \left\{ (f_{\frac{7}{2}})_{T=1}^2 \left[ (d_{\frac{3}{2}})_{T=\frac{3}{2}}^{-3} (s_{\frac{1}{2}})^{-1} \right]_{J=2} \right\}_{T=0} \right\}_{J=2} \right.$$

These states contain no spurious center-of-mass motion. We have used the relevant experimental binding and excitation energies and calculated the particle-hole interaction using the matrix elements of Kuo and Brown <sup>27</sup>), which were derived from realistic forces with corrections appropriate to a  $^{40}\text{Ca}$  core. Use of the empirical matrix elements of Ern e <sup>28</sup>) or Dieperink and Brussaard <sup>29</sup>), or the interaction of Zamick <sup>25</sup>) for the diagonal elements, would result in little change.

The mixing of the two-hole and 2p-4h states is largely determined by the matrix element  $\langle d_{\frac{3}{2}}^2 J = 0 | V | f_{\frac{7}{2}}^2 J = 0 \rangle$ . Gerace and Green <sup>26</sup>) adopt a value of 3.1 MeV for this quantity and Kuo and Brown <sup>27</sup>) give a value of 2.6 MeV. However, these values would result in a  $0_1^+ - 0_2^+$  splitting of over 5 MeV. We have therefore used the

value of 1.6 MeV given by the Kallio-Kolltveit potential using the relative coordinate matrix elements of Zamick and Mavromatis quoted by Bertsch<sup>30</sup>).

The resulting energy levels are given in fig. 8, where we have used the two-hole matrix elements generated by the Yukawa potential. The spectroscopic factors and the intensities of the core-excited states are listed at the right in table 5. The spectroscopic factors of the  $2_2^+$  and  $2_3^+$  states are somewhat larger than the experimental numbers for the 3.94 and 4.57 MeV levels, in roughly the same proportion. Also it would be desirable to increase the value of  $C^2S_0$  for the  $2_4^+$  level (at the expense of the  $2_3^+$ ) if we are to identify it with the 5.16 MeV level. This level definitely has  $J^\pi = 2^+$  since it is also observed in the  $^{40}\text{Ar}(p, t)^{38}\text{Ar}$  reaction<sup>31</sup>), indicating natural parity. The level at 5.56 MeV remains as the best candidate for the two-hole  $1_1^+$  level.

In order to estimate the effect of core excitation in  $^{39}\text{K}$  on the spectroscopic factors for the  $0^+$  and  $2^+$  states, a state of the form

$$\left\{ \left( f_{\frac{1}{2}} \right)_{J=0}^2 \left( d_{\frac{3}{2}} \right)_{J=\frac{3}{2}}^{-3} \right\}_{J=\frac{3}{2}}_{T=\frac{1}{2}}$$

was allowed to mix into the  $^{39}\text{K}$  ground state. The result is about 12 % mixing, with appreciable changes in the spectroscopic factors only for the  $2_2^+$  level ( $C^2S_2 = 0.15$  instead of 0.32) and the  $2_3^+$  level ( $C^2S_0 = 0.66$  instead of 0.80). Also  $C^2S_2$  for the  $0_2^+$  is reduced from 0.03 to 0.00. These changes all improve agreement between theory and experiment.

For the  $\gamma$  transitions given in table 6 we have used a neutron effective charge  $e_n$  of unity and a proton effective charge  $e_p$  of 1.5, which Gerace and Green found reasonable<sup>26</sup>). A value of one for  $e_p$  was also tried and this seems to give somewhat better results. Reduction of the neutron effective charge is not indicated since it would reduce the  $2_2^+ \rightarrow 0_1^+ B(E2)$  further below the experimental value. The use of a value of  $e_n$  larger than  $(e_p - 1)$  has some theoretical justification<sup>32,33</sup>).

The agreement between experiment and theory for the  $2_2^+ \rightarrow 2_1^+$  transition has been improved relative to the two-hole calculation. The branching ratio for this transition has been taken to be  $< 4\%$  from the work of Engelbertink *et al.*<sup>34</sup>), although Röpke *et al.*<sup>35</sup>) find a somewhat larger branch of  $10 \pm 5\%$ . Taking the latter value would improve the agreement between theory and experiment. Comparing the decay of the  $2_3^+$  to that of the 4.57 MeV level, we find too large a  $B(E2)$  to the ground state and also too large a  $B(M1)$  for the transition to the  $2_2^+$ . However, Engelbertink *et al.*<sup>34</sup>) find that the 4.57 MeV level is fed by the  $4^-, T = 2$  level at 11.93 MeV. The corresponding  $4^-$  level in  $^{38}\text{Cl}$  has been assigned to the  $(f_{\frac{1}{2}})(d_{\frac{3}{2}})^{-3}$  configuration<sup>23,28</sup>), so that a transition from the 11.93 MeV level to our  $2_3^+$  would be expected to proceed only through the small  $(d_{\frac{3}{2}})^{-2}$  component. We would therefore expect the M2 transition to be unfavored, yet the measured width gives  $|M|^2 = 29$  W.u. Thus it seems possible that there are two levels at approximately this energy, one with the  $J^\pi = (2^-)$  assignment of ref. <sup>34</sup>) and the other with  $J^\pi = (1, 2)^+$  found here. Confirmation of a level at 4.57 MeV with positive parity is provided by the

$^{37}\text{Cl}(^3\text{He}, d)^{38}\text{Ar}$  reaction <sup>24</sup>). The excitation energy of this level is given in ref. <sup>24</sup>) as  $4.566 \pm 0.008$  MeV, in good agreement with the value  $4.569 \pm 0.010$  MeV measured in the present ( $d, ^3\text{He}$ ) experiment. We also note that a level at approximately this energy is strongly excited in the  $^{40}\text{Ar}(p, t)^{38}\text{Ar}$  reaction <sup>31</sup>), indicating natural parity. Since the nearby  $5^-$  is expected to be populated weakly, this would appear to argue

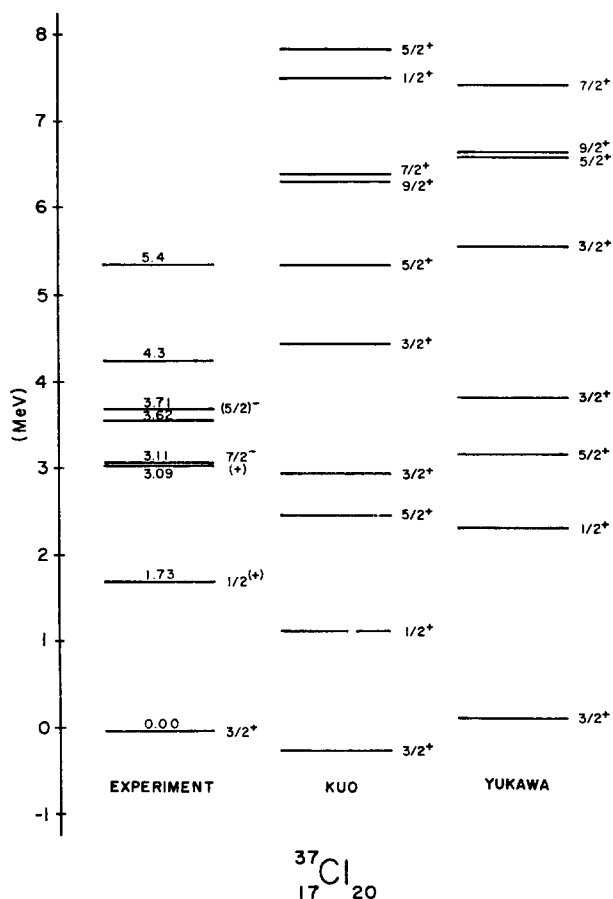


Fig. 9. Comparison of the experimentally determined levels of  $^{37}\text{Cl}$  with the results of the three-hole calculations. The vertical scale represents the absolute interaction energies, *i.e.*, the ground state energy is  $3[\text{B.E.}(^{39}\text{K}) - \text{B.E.}(^{40}\text{Ca})] - [\text{B.E.}(^{37}\text{Cl}) - \text{B.E.}(^{40}\text{Ca})]$ .

in favour of our suggestion of  $2^+$  and would certainly exclude ( $2^-$ ). The decay properties of the 5.36 MeV  $2^+(1^+)$  level <sup>35</sup>), not observed in the present experiment, would not be consistent with those of the  $2_4^+$ , which is expected to decay largely by M1 radiation to the  $2_2^+$  and  $2_3^+$  levels.



5.4. THE STRUCTURE OF  $^{37}\text{Cl}$  AND  $^{36}\text{S}$ 

The three-hole spectrum of  $^{37}\text{Cl}$  is compared with experiment <sup>1,36)</sup> in fig. 9 and the results seem to be quite reasonable. It is interesting to note that Glaudemans

TABLE 7  
Configuration intensities for levels in  $^{37}\text{Cl}$  and  $^{36}\text{S}$

$^{37}\text{Cl}$							
$J^\pi$	$d_{\frac{3}{2}}^{-3}$	$d_{\frac{3}{2}}^{-2} s_{\frac{3}{2}}^{-1}$	$d_{\frac{3}{2}}^{-1} s_{\frac{3}{2}}^{-2}$	$d_{\frac{3}{2}}^{-2} d_{\frac{3}{2}}^{-1}$	$(d_{\frac{3}{2}}, s_{\frac{3}{2}})^{-2} d_{\frac{3}{2}}^{-1}$ <sup>a)</sup>	$(d_{\frac{3}{2}}, s_{\frac{3}{2}})^{-1} d_{\frac{3}{2}}^{-2}$	
$\frac{1}{2}_1^+$		91		1	4	4	
$\frac{3}{2}_1^+$	91	1	3	1	1	4	
$\frac{3}{2}_2^+$	1	18	77	0	3	1	
$\frac{3}{2}_3^+$	3	70	20	0	6	0	
$\frac{5}{2}_1^+$		92		1	7	1	
$\frac{5}{2}_2^+$		1		91 <sup>b)</sup>	95	2	
$\frac{7}{2}_1^+$				94	95	5	
$\frac{9}{2}_1^+$				97	99	1	
$^{36}\text{S}$							
$J^\pi$	$d_{\frac{3}{2}}^{-4}$	$d_{\frac{3}{2}}^{-3} s_{\frac{3}{2}}^{-1}$	$d_{\frac{3}{2}}^{-2} s_{\frac{3}{2}}^{-2}$	$d_{\frac{3}{2}}^{-3} d_{\frac{3}{2}}^{-1}$	$(d_{\frac{3}{2}}, s_{\frac{3}{2}})^{-3} d_{\frac{3}{2}}^{-1}$ <sup>a)</sup>	$(d_{\frac{3}{2}}, s_{\frac{3}{2}})^{-2} d_{\frac{3}{2}}^{-2}$	
$0_1^+$	84		7		0	9	
$0_2^+$	8		86		1	6	
$1_1^+$		88		0	9	3	
$2_1^+$		82	7	0	7	4	
$2_2^+$		7	88	0	2	2	
$2_3^+$		0	1	70	87	10	
$3_1^+$				89	95	4	
$4_1^+$				91	94	3	

<sup>a)</sup> Includes preceding column.

<sup>b)</sup> Mostly seniority 1.

*et al.* <sup>17)</sup> predict the  $\frac{3}{2}_2^+$  and  $\frac{3}{2}_3^+$  much higher at 4.9 and 6.4 MeV excitation energy. The intensities of the configurations present in the low-lying states of  $^{37}\text{Cl}$  and  $^{36}\text{S}$  are given in table 7 for the Yukawa case. For the Kuo case the results are very similar, apart from the  $\frac{3}{2}_2^+$  and  $\frac{3}{2}_3^+$  states, which have the percentages of  $(d_{\frac{3}{2}})^{-2}(s_{\frac{3}{2}})^{-1}$  and  $(d_{\frac{3}{2}})^{-1}(s_{\frac{3}{2}})^{-2}$  reversed. The difference is due mainly to the diagonal  $(d_{\frac{3}{2}})(s_{\frac{3}{2}})$  matrix element for  $J = 1$ , which is more repulsive in the Yukawa case.

The four-hole spectrum of  $^{36}\text{S}$  is compared with experiment in fig. 10 and the

spectroscopic factors are given in table 8. The ground state is somewhat overbound in the Kuo case and underbound with the Yukawa interaction. The predicted spectroscopic factor agrees quite well with experiment. The  $0^+$  and  $2^+$  levels at 2.0 and 2.9 MeV excitation energy were not observed in the present experiment and presumably correspond to core-excited states. Using the methods of subsect. 5.3 the lowest such

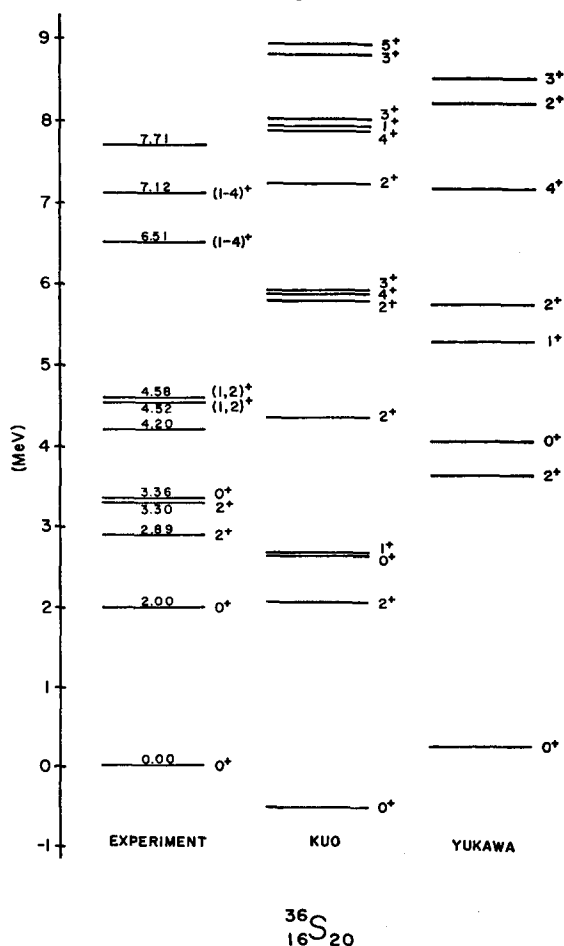


Fig. 10. Comparison of the experimentally determined levels of  $^{36}\text{S}$  with the results of the four-hole calculations. The vertical scale represents the absolute interaction energies, *i.e.*, the ground state energy is  $4[\text{B.E.}(^{39}\text{K})-\text{B.E.}(^{40}\text{Ca})]-[\text{B.E.}(^{36}\text{S})-\text{B.E.}(^{40}\text{Ca})]$ .

state is expected to be a  $0^+$ ,  $2p-6h$  state with both the particles and holes coupled to  $T = 1$ . This fits in nicely with the observation of these levels in the  $^{34}\text{S}(t, p)^{36}\text{S}$  reaction <sup>1</sup>). The theoretical weak-coupling estimate of the energy is 3.5 MeV, which is rather high. Ern e <sup>28</sup>) has calculated a similar value. There is another  $0^+$  level at 3.36 MeV which is seen in the  $(t, p)$  but not the  $(d, ^3\text{He})$  reaction. We have tentatively identified this with the theoretical  $0_2^+$ , which has a small value of  $C^2S$ .

TABLE 8  
Comparison of experimental and theoretical spectroscopic factors for the  $^{37}\text{Cl}(d, ^3\text{He})^{36}\text{S}$  reaction

Level	Experiment <sup>a, b)</sup>		$J^\pi$	Theory	
	$C^2S_0$	$C^2S_2$		$C^2S_0$	$C^2S_2$
G.S., $0^+$		1.06	$0_1^+$	0	0.90
2.00, $0^+$		<0.05			
2.89, $2^+$	<0.01	<0.03			
3.30, $2^+$ <sup>c)</sup>	0.86		$2_1^+$	1.07	0.00
3.36, $0^+$		<0.10	$0_2^+$	0	0.03
4.20 <sup>b)</sup>					
4.52(1, 2) <sup>+</sup>	0.75		$1_1^+$	0.68	0.02
4.58(1, 2) <sup>+</sup>	0.25		$2_2^+$	0.04	0.09
6.51(1-4) <sup>+</sup>		0.19			
7.12(1-4) <sup>+</sup>		0.44			
			$4_1^+$	0	2.12
			$2_3^+$	0.00	0.96
			$3_1^+$	0	1.59

<sup>a)</sup> Present work.

<sup>b)</sup> Ref. <sup>1)</sup>.

<sup>c)</sup> See text.

The level at about 3.30 MeV is identified in this experiment as  $(1, 2)^+$  and the (t, p) work of Hinds and Middleton (see ref. <sup>1)</sup>), indicates that it has natural parity. This establishes a  $J^\pi$  of  $2^+$ , and we identify it with the theoretical  $2_1^+$ , although the spectroscopic factor is somewhat smaller than theory predicts. The only other large value of  $C^2S_0$  occurs for the lower member of the doublet at  $\approx 4.5$  MeV, which presumably should be identified with the  $1_1^+$ . The predicted value of  $C^2S_0$  for this level is then in good agreement with experiment. The identity of the upper member of the doublet is not clear, since the  $C^2S_0$  is much larger than that predicted for the  $2_2^+$ . However the sum of  $C^2S_0$  values for the states at 3.295 and 4.577 MeV corresponds closely to the sum predicted for the  $2_1^+$  and  $2_2^+$  levels and it may be that the inclusion of core-excited states would alter the distribution of strength. It may also be important to include such states in computing the excitation energies, since neither of our interactions gives a good fit. The Yukawa interaction gives the better result for the  $1_1^+$  energy due to the diagonal  $(d_{\frac{3}{2}})(s_{\frac{3}{2}})_{J=1}$  matrix element, which has the value 1.4 MeV compared to 0.2 MeV for the Kuo case. Thus it appears that stronger repulsion in triplet-odd states is needed at the end of the 2s-1d shell, although we have probably overestimated this somewhat. Glaudemans *et al.* <sup>17)</sup> take a value of 1.8 MeV for this matrix element and consequently predict the  $1^+$  state at 5.8 MeV. Note that if

we modify the matrix element to fit the probable  $1_1^+$  in  $^{38}\text{Ar}$ , the  $1_1^+$  in  $^{36}\text{S}$  lies too low.

The levels at 6.511 and 7.12 MeV are observed in this experiment by  $l = 2$  transfer. Since the  $d_{3/2}$  strength is exhausted by the ground state transition, the only other candidates for appreciable  $l = 2$  strengths are the states with large fractions of the  $(d_{3/2})^{-3}(d_{3/2})^{-1}$  configuration. As was the case for the 7.14 MeV level in  $^{38}\text{Ar}$ , the experimental  $C^2S_2$  values are much less than predicted for the  $d_{3/2}$  hole states, presumably because the strength is fragmented into many levels which were not detected.

## 6. Summary

The  $^{37}\text{Cl}(d, ^3\text{He})^{36}\text{S}$  and  $^{39}\text{K}(d, ^3\text{He})^{38}\text{Ar}$  reactions have been used to investigate 2s-1d hole states in  $^{36}\text{S}$  and  $^{38}\text{Ar}$ . The spectroscopic factors for the transitions to the ground state and first excited  $2^+$  state of  $^{38}\text{Ar}$  are in agreement with theoretical predictions describing these states as formed by two holes in the  $^{40}\text{Ca}$  core. However, four strong  $l = 0$  transitions are observed to  $(1, 2)^+$  levels at 3.935, 4.569, 5.158 and 5.563 MeV in  $^{38}\text{Ar}$ , while only two transitions with appreciable  $l = 0$  strength would be expected on the basis of the two-hole model. When 2p-4h excitations of the  $^{40}\text{Ca}$  core are considered, the data suggest that the 3.935 and 4.569 MeV levels are largely 2p-4h and two-hole respectively, both with  $J^\pi = 2^+$ , and that the 5.563 MeV level corresponds to the  $1^+$  member of the  $(d_{3/2})^{-1}(s_{1/2})^{-1}$  configuration. Since the level at 5.158 MeV is clearly seen in the  $^{40}\text{Ar}(p, t)^{38}\text{Ar}$  reaction<sup>31)</sup>, it must have natural parity and hence  $J^\pi = 2^+$  is established.

The transition to the ground state of  $^{36}\text{S}$  is observed with a value of  $C^2S_2(d_{3/2})$  in reasonable accord with the predictions of a four-hole model. Three  $l = 0$  transitions have been identified leading to levels at 3.295, 4.523, and 4.577 MeV in  $^{36}\text{S}$ , which can therefore be assigned  $(1, 2)^+$ . The level at 3.295 MeV corresponds to the  $(2^+, 3^-)$  level reported<sup>1)</sup> at 3.304 MeV from the  $^{34}\text{S}(t, p)^{36}\text{S}$  reaction. An assignment of  $J^\pi = 2^+$  for this level is therefore established. The spectroscopic factor for the 4.523 MeV level is then in accord with theoretical predictions for a  $1^+$  state belonging largely to the  $(d_{3/2})^{-3}(s_{1/2})^{-1}$  configuration. The 4.577 MeV level may have  $J^\pi = 2^+$ , but the spectroscopic factor is larger than theory suggests.

Some  $l = 2$  strength has been observed leading to levels at about 7 MeV excitation energy in  $^{36}\text{S}$  and  $^{38}\text{Ar}$ , but the spectroscopic factors are smaller than those calculated for states with mainly one  $d_{3/2}$  hole. This probably indicates that such states are fragmented along several levels but does suggest that a  $d_{3/2}$ - $d_{3/2}$  splitting as large as 7.5 MeV is required.

The authors are indebted to Professor K. T. Hecht for many valuable discussions and to Dr. J. C. Hardy for communicating to us prior to publication his results from the  $^{40}\text{Ar}(p, t)^{38}\text{Ar}$  reaction. The use of computer codes written by Dr. T. England is gratefully acknowledged. We are grateful to Professor P. D. Kunz for making the code DWUCK available to use and to K. A. Erb for making modifications needed to allow use of the code with the IBM 360 computer. We also wish to thank

H. Grunder for performing the spectrophotometric analysis of the potassium target material.

*Note added in proof:* For the  $^{38}\text{Ar } 2.17 \text{ } 2^+ \text{ to g.s. } 0^+ \text{ } \gamma$  transition we have quoted a  $B(E2)$  of  $25 \pm 4 \text{ } e^2 \cdot \text{fm}^4$  derived from the results of Grawe and Lieb mentioned in ref. <sup>23)</sup>. A recent publication by these authors <sup>37)</sup> leads to a larger  $B(E2)$  value of  $40 \pm 10 \text{ } e^2 \cdot \text{fm}^4$ . This is in substantial disagreement with the limit  $B(E2) \leq 17 \text{ } e^2 \cdot \text{fm}^4$ , derived from ref. <sup>1)</sup> and hence it seems difficult to draw any firm conclusions regarding this transition.

### References

- 1) P. M. Endt and C. van der Leun, Nucl. Phys. **A105** (1967) 1
- 2) W. S. Gray, T. Wei, J. Jänecke and R. M. Polichar, Phys. Lett. **26B** (1968) 383
- 3) N. C. Puttaswamy and J. L. Yntema, Phys. Rev. **177** (1969) 1624
- 4) B. H. Wildenthal and E. Newman, Nucl. Phys. **A118** (1968) 347
- 5) T. Wei, W. S. Gray, J. Jänecke and R. M. Polichar, Bull. Am. Phys. Soc. **12** (1967) 681
- 6) W. C. Parkinson, R. S. Tickle, P. Bruinsma, J. Bardwick and J. M. Lambert, Nucl. Instr. **18** (1962) 93
- 7) P. D. Kunz, unpublished
- 8) M. H. Macfarlane and J. B. French, Revs. Mod. Phys. **32** (1960) 567
- 9) R. H. Bassel, Phys. Rev. **149** (1966) 791
- 10) E. Newman, L. C. Becker, B. M. Freedman and J. C. Hiebert, Nucl. Phys. **A100** (1967) 225
- 11) E. F. Gibson, B. W. Ridley, J. J. Kraushaar, M. E. Rickey and R. H. Bassel, Phys. Rev. **155** (1967) 1194
- 12) L. L. Lee, Jr., J. P. Schiffer, B. Zeidman, G. R. Satchler, R. M. Drisko and R. H. Bassel, Phys. Rev. **136** (1964) B971
- 13) J. C. Hiebert, E. Newman and R. H. Bassel, Phys. Rev. **154** (1967) 898
- 14) P. J. A. Buttle and L. J. B. Goldfarb, Proc. Phys. Soc. **83** (1964) 701;  
F. G. Perey and D. Saxon, Phys. Lett. **10** (1964) 107;  
G. Y. Bencze and J. Z. Zimányi, Phys. Lett. **9** (1964) 246;  
F. G. Perey and A. M. Saruis, Nucl. Phys. **70** (1965) 225
- 15) Kamal K. Seth, J. A. Biggerstaff, P. D. Miller and G. R. Satchler, Phys. Rev. **164** (1967) 1450
- 16) B. M. Freedman, E. Newman and J. C. Hiebert, Phys. Rev. **166** (1968) 1156
- 17) P. W. M. Glaudemans, G. Wiechers and P. J. Brussaard, Nucl. Phys. **56** (1964) 529 and 548
- 18) B. H. Wildenthal and E. Newman, Phys. Rev. **175** (1968) 1431
- 19) Y. Akiyama, Nucl. Data **A2** (1966) 403
- 20) J. D. Vergados, Nucl. Phys. **A111** (1968) 681
- 21) H. A. Jahn and H. Van Wieringen, Proc. Roy. Soc. **A209** (1951) 502
- 22) T. T. S. Kuo, Nucl. Phys. **A103** (1967) 71
- 23) G. A. P. Engelbertink and P. W. M. Glaudemans, Nucl. Phys. **A123** (1969) 225
- 24) M. A. Moinester and W. P. Alford, preprint
- 25) L. Zamick, Phys. Lett. **19** (1965) 580
- 26) W. J. Gerace and A. M. Green, Nucl. Phys. **A93** (1967) 110
- 27) T. T. S. Kuo and G. E. Brown, Nucl. Phys. **A114** (1968) 241
- 28) F. C. Erné, Nucl. Phys. **84** (1966) 91
- 29) A. E. L. Dieperink and P. J. Brussaard, Nucl. Phys. **A106** (1968) 177
- 30) G. Bertsch, Nucl. Phys. **79** (1966) 209
- 31) J. C. Hardy, H. Brunnader and J. Cerny, Phys. Rev., to be published
- 32) H. Horie and A. Arima, Phys. Rev. **99** (1955) 778
- 33) P. Federman and L. Zamick, Phys. Rev. **177** (1969) 1534
- 34) G. A. P. Engelbertink, H. Lindeman and M. J. N. Jacobs, Nucl. Phys. **A107** (1968) 305
- 35) H. Röpke, K. P. Lieb and H. Brundiers, Nucl. Phys. **A104** (1967) 529
- 36) S. Wirjoamidjojo and B. D. Kern, Phys. Rev. **163** (1967) 1094
- 37) H. Grawe and K. P. Lieb, Nucl. Phys. **A127** (1969) 13